

# Thermal Behavior and Micro Structure of TKX-50

Michael Herrmann<sup>\*[a]</sup> and Ulrich Förter-Barth<sup>[a]</sup>*Dedicated to Professor Dr. Thomas M. Klapötke on the Occasion of his 60th Birthday*

**Abstract:** The thermal behaviour of TKX-50 was re-investigated in an extended temperature range by means of temperature resolved X-ray diffraction. TKX-50, synthesized at the Fraunhofer ICT, was identified using Rietveld-analysis and reference data from the CCDC. Monitoring the refined crystal data versus temperature verified a highly anisotropic expansion behavior connected to a layer structure. However, the coefficients of thermal expansion (CTEs) were found at an order of magnitude higher than reported, and a slight bent of lattice parameter *a* was found near room temperature. At temperatures between 180 and

200 °C the decomposition of TKX-50 started with the formation of 1 to 5 wt.% diammonium 5,5'-bistetrazole-1,1'-diolate (ABTOX). Moreover, the micro structure was investigated by means of size/strain analysis and so called indexed Williamson-Hall plot. The analysis revealed moderate micro strain and absence of size broadening. The results give rise to the hypothesis that the (010) layer structure supports a low sensitivity of TKX-50 without impairment of the mechanical stability. The results provide a base for future quality assessment and the development of advanced products.

**Keywords:** TKX-50 · X-ray diffraction · Thermal expansion · Micro structure

## 1 Introduction

TKX-50 (C<sub>2</sub>H<sub>8</sub>N<sub>10</sub>O<sub>4</sub>, dihydroxylammonium 5,5'-bistetrazole-1,1'-diolate) is a promising, powerful new energetic material. It is easily prepared, insensitive, lowly toxic, and proposed to replace RDX [1–3]. The crystal structure and thermal behavior of TKX-50 was reported by Fischer et al. in 2012 [1] and crystal structure data was deposited at the Cambridge Crystallographic Data Centre [CCDC 872231 and 872232]. TKX-50 crystallizes in the monoclinic space group P2<sub>1</sub>/c with two anion-cation moieties in the unit cell and with a density of 1.877 g cm<sup>-3</sup> at 298 K.

Applying DSC, the authors did not find exothermic or endothermic events below the decomposition with an onset at 222 °C [1]. Further investigations revealed that a two-step decomposition starts at 210–250 °C depending on the heating rate, preceded by an endothermic low enthalpy process in the range 130–200 °C. The preceding process was suspected to represent a phase transformation or some form of structural rearrangement [4]. Lu et al. [5] reported a solid-solid phase transition to a metastable phase (Meta-TKX-50) at about 180 °C, which was detected with Raman spectroscopy and TGA-DSC. The authors concluded that Meta-TKX-50 is formed by the rotation of NH<sub>3</sub>OH<sup>+</sup> with 3% volume expansion, a crystal symmetry reduction from P2<sub>1</sub>/c to P-1, and a slight change of specific heat capacity. The latter shall be the main reason that the phase transition was overlooked in past measurements.

Temperature resolved powder XRD measurements performed by Jia et al. [6] revealed an anisotropic thermal expansion of TKX-50 with a negative thermal expansion coefficient (CTE) of the lattice parameter *a*. The contraction

was attributed to a distortion of the six-membered ring resulting in H-transfer between the cation and di-anion. Besides, changes in diffraction patterns were monitored up to six hours at temperatures between 190 and 198 °C with in situ isothermal X-ray diffraction. The investigations revealed primary decomposition of TKX-50 with an emerging intermediate product diammonium 5,5'-bitetrazole-1,1'-diolate (ABTOX, CCDC 1567754).

The structural response of TKX-50 under high pressure up to 10 GPa was examined by Dreger et al. [7] by means of synchrotron single-crystal X-ray diffraction. The investigations revealed a highly anisotropic compression and a significantly lower volume compressibility than in currently known energetic crystals. Additionally, anomalous compression with even an expansion of the lattice parameter *a* upon compression to ~3 GPa was reported. The authors concluded that the structural stability of TKX-50 is controlled by strong and highly anisotropic intermolecular interactions, which may contribute to its shock insensitivity.

TKX-50 is synthesized at the Fraunhofer ICT up to kg quantities and its compatibility with HTPB, paraffin, wax,

[a] M. Herrmann, U. Förter-Barth  
Fraunhofer Institute for Chemical Technology ICT  
D-76327 Pfinztal, Germany  
\*e-mail: michael.herrmann@ict.fraunhofer.de

© 2021 The Authors. Propellants, Explosives, Pyrotechnics published by Wiley-VCH GmbH. This is an open access article under the terms of the Creative Commons Attribution Non-Commercial License, which permits use, distribution and reproduction in any medium, provided the original work is properly cited and is not used for commercial purposes.

GAP, hexogen, aluminum and isocyanates was tested. Furthermore, TKX-50/paraffin wax/graphite charges were pressed and characterized in detonation tests [8]. The substance is still in the focus of current investigations with the object of developing new high-performance low sensitivity energetic formulations. In this context the thermal behavior of TKX-50 was reinvestigated by means of temperature resolved X-ray diffraction. The measurements include also temperatures below room temperature (down to  $-80^{\circ}\text{C}$ ) and high temperatures up to  $200^{\circ}\text{C}$ . Moreover, the micro structure of TKX-50 was investigated by size/strain analysis and Williamson Hall-Plot. Hence, the results provide a base for future quality assessment and shall help to the develop products including high quality TKX-50 crystals.

## 2 Experimental Section

TKX-50 samples were measured with a Bragg-Brentano diffractometer D8 Advance from Bruker AXS equipped with copper tube, Ni filter, two  $2.5^{\circ}$  Soller collimators, variable V6 divergence slit, a temperature device from MRI, and a silicon strip detector with  $3^{\circ}2\theta$  detector opening. Diffraction patterns were monitored between  $12$  and  $50^{\circ}2\theta$  with  $0.05^{\circ}2\theta$  step width and three seconds counting time per step. Temperatures were hold constant while capturing the diffraction patterns ( $\sim 40$  min), and were increased linearly in temperature steps of  $20$  K with  $12$  K/min heating rate. Temperature cycling were performed due to the program  $20/-80/200^{\circ}\text{C}$ . Additionally, room temperature measurements were performed with a standard sample holder and anti-scatter aperture between  $10$  and  $60^{\circ}2\theta$  with  $0.02^{\circ}2\theta$  step width. Besides, the standard reference material SRM 660a [9] was measured under the same conditions and the geometric peak broadening was parametrized using the modified Pseudo-Voigt profile.

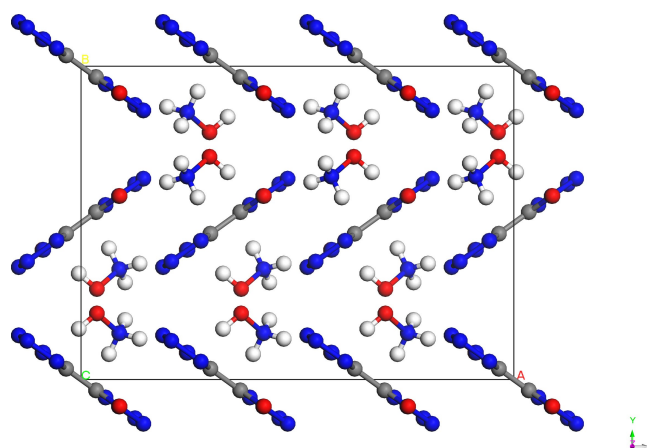
The diffraction patterns were evaluated by means of Rietveld-analysis [10] using the program TOPAS from Bruker AXS [11] and the crystal structure reported by Fischer et al. [1]. The evaluation yields refined lattice parameters, the mean volume-weighted domain size (LVol-FWHM) and mean micro strain ( $\epsilon_0$ ) of TKX-50 at room temperature. The lattice parameters were plotted versus temperature and the coefficients of thermal expansion (CTEs) were determined by means of regression lines. Furthermore, the anisotropic diffraction peak broadening was characterized by means of so-called Williamson-Hall plots [12, 13]. Therefore, reciprocal peak widths  $\beta^* = \beta/\lambda \cos \theta$  are plotted versus reciprocal lattice distances  $d^* = 2/\lambda \sin \theta$ , where  $\beta$ ,  $d$ ,  $2\theta$  and  $\lambda$  are the diffraction line widths, lattice distances, diffraction angles and the wavelength of the X-ray radiation.

## 3 Results and Discussion

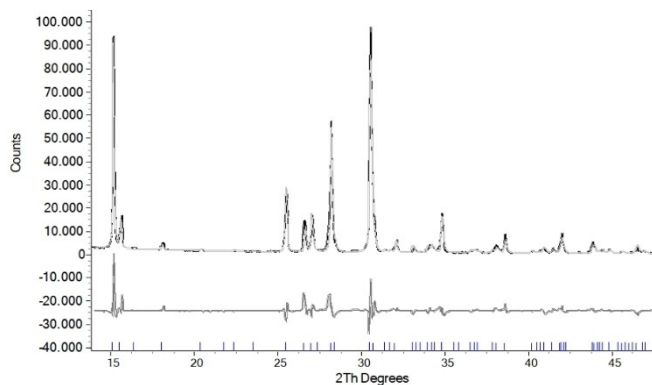
### 3.1 Crystal Structure

Figure 1 depicts three elementary cells of TKX-50, which were generated using the crystal data reported by Fischer et al. [1]. The ions arrange within (horizontal) layers parallel to the (010) plane. The shortest H-bonds with  $1.714$  Å and  $2.184$  Å occur within these layers followed by H-bond lengths of  $2.359$  Å and  $2.497$  Å between the layers.

X-ray diffraction measurements identified the expected crystal structure by comparison with calculated patterns of the crystal structure data of CCDC 872232 (298 K), but yielded strongly enhanced intensities of the reflection (020), (040), and (060). The differences represent a preferred orientation of crystals, which is typical e.g. for platelets that orientate parallel to the sample surface during preparation. Comparing the preferred orientation to the model in Figure 1 revealed that during crystallization TKX-50 crystals grew fast along the (010) layers, but slowly perpendicular to the (010) crystal faces. Hence, samples were ground in order to reduce the preferred orientation during sample preparation. Moderate Rietveld fits were achieved with the ground samples (e.g. Figure 2), but still with some differences of the peak intensities at  $15.13^{\circ}2\theta$  (020) and  $30.52^{\circ}2\theta$  (040) and a slight misfit of the peak (031) at  $26.62^{\circ}2\theta$ . The refinement eventually resulted in a weighted pattern error of 18.2 and 19.9, when using CCDC 872231 and 872232, respectively. Refined lattice parameters of  $a$ ,  $b$ ,  $c$ , and  $\beta$  were  $5.439$  Å,  $11.720$  Å,  $6.546$  Å, and  $95.09^{\circ}$ , respectively, and the crystal density was calculated to  $1.887$  g cm $^{-3}$ , which is slightly higher than the reference value of  $1.877$  g cm $^{-3}$  given in CCDC 872232 (Table 1). The micro structure analysis yielded a volume-weighted domain size of  $5.4$  μm and a micro strain value  $\epsilon_0$  of 0.00033. That means that approx-



**Figure 1.** Schematic drawing of TKX-50 with three elementary cells and the arrangement of the cations and anions. The drawing is based on the crystal structure data reported by Fischer et al. [1]. View is along the  $z$  axis.



**Figure 2.** X-ray diffraction pattern of TKX-50 (black), fitted pattern (light grey), differences (grey) and position marker of the calculated structure (bottom).

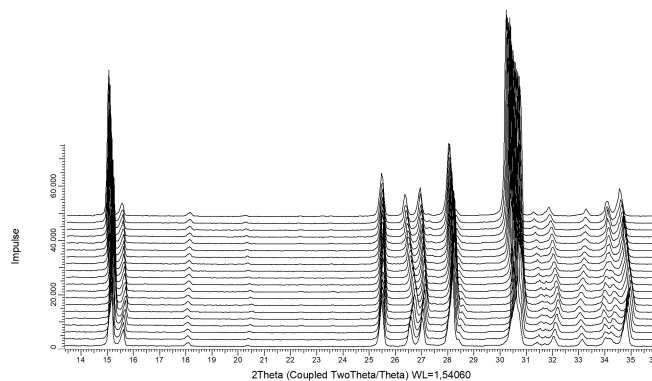


**Figure 3.** Section of a waterfall plot of diffraction patterns of TKX-50 measured with the temperature program 20/–80/200 °C with 20 °C steps (bottom to top).

**Table 1.** Reported and measured crystal structure data of TKX-50.

	CCDC 872231	CCDC 872232	this work
Temperature, [K]	100(2)	298	293
Lattice parameters			
a, [Å]	5.4872(8)	5.4408(6)	5.439
b, [Å]	11.5472(15)	11.7514(13)	11.720
c, [Å]	6.4833(9)	6.5612(9)	6.546
β, [°]	95.402(12)	95.071(11)	95.09
Cell volume, [Å <sup>3</sup> ]	408.97(10)	417.86(9)	415.7
Density, [g cm <sup>-3</sup> ]	1.918	1.877	1.887
Domain Size, [μm]	–	–	5.42
Micro strain, [ ]	–	–	0.00033

imately no size broadening of diffraction peaks occurred in the TKX-50 sample but a moderate micro strain.

### 3.2 Thermal Expansion of TKX-50

The waterfall plot of Figure 3 depicts diffraction patterns of TKX-50 measured with the temperature program 20/–80/200 °C (bottom to top). Peak shifts represent the thermal expansion and contraction of the crystal structure during cooling and heating. The bend at the sixth lowest pattern represents the minimum of the temperature cycle at –80 °C. A phase transition, which would be identified by disappearing and emerging new peaks, was not detected.

The lattice parameters of TKX-50 are plotted versus temperature in the Figures 4 and 5 and the relative linear coefficients of thermal expansion (CTEs) are summarized in Table 2. The TKX-50 structure expands anisotropically with a strong thermal expansion of the lattice parameter *b* with  $7.242 \cdot 10^{-5} \text{ K}^{-1}$ , a medium expansion of *c* with  $4.197 \cdot 10^{-5} \text{ K}^{-1}$  versus a slightly contracting lattice parameter *a* with negative CTE of  $-1.734 \cdot 10^{-5} \text{ K}^{-1}$ . As lattice parameter *a* runs through a slight bent at ~50 °C, the CTEs of the left and the right branch were evaluated separately, which resulted in a

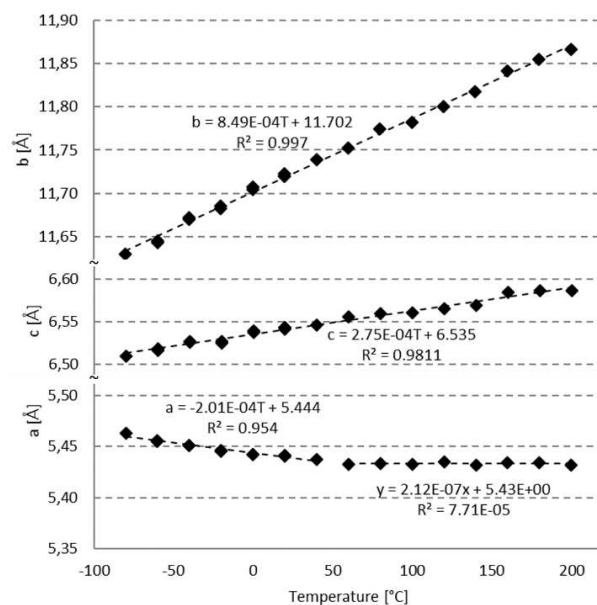


**Figure 4.** Lattice parameters *a*, *b*, *c* of TKX-50, monitored during cycling between –80 and 200 °C.

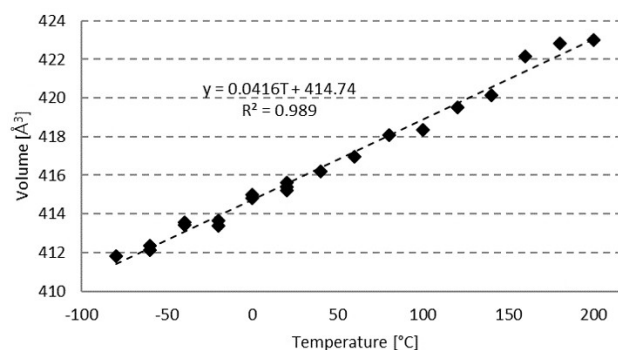


**Figure 5.** Volume of the elementary cell of TKX-50, monitored during cycling between –80 and 200 °C.

**Table 2.** Coefficients of thermal expansion (CTEs\*) of TKX-50.

Lattice parameter	this work [ $10^{-5} \text{ K}^{-1}$ ]	Jia et al. [6] [ $10^{-6}$ ]
a	−1.734	−1.04635
< 50 °C	−3.689	
> 50 °C	0.004	
b	7.242	5.56149
c	4.197	4.76293
$\beta$	−1.860	−1.92479
spec. Vol.	9.996	2.2973

\* evaluated relative to the primary value at room temperature

highly negative CTE of  $-3.689 \cdot 10^{-5} \text{ K}^{-1}$  in the low temperature region and an approximately constant parameter above 50 °C. Quantitative analysis of the patterns revealed a concentration of 1 wt% of the intermediate decomposition product ABTOX (CCDC 1567754) at 200 °C and 5 wt% after cooling to room temperature. So far, the investigations showed qualitatively the same thermal behavior as reported by Jia et al. [6] (Table 2), but monitor also the temperature range between room temperature and  $-80 \text{ °C}$  and high temperatures up to 200 °C. The most striking difference however is that the CTEs are found at about one order of magnitude higher as reported. Moreover, a slight bent of a lattice parameter was observed, the latter became visible through the extended temperature range, and micro structure parameters, related to the internal crystal quality, were determined at room temperature.

### 3.3 Anisotropic Peak Broadening

Figure 6 depicts a calibrated indexed Williamson-Hall plot of TKX-50. For interpretation the following properties of

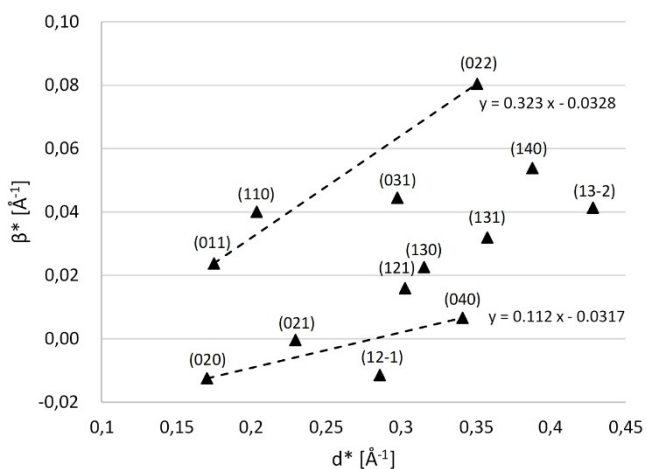


**Figure 6.** Indexed Williamson-Hall plot of TKX-50 at room temperature.

Williamson-Hall plots are considered. Provided that crystallite size or micro strain would be isotropic and no strain broadening occurred, the reciprocal peak widths ( $\beta^*$ ) would lie on a horizontal line intercepting the y-axis at the inverse of the mean linear crystallite size  $t$ . In the same case but without size broadening the values would lie on a straight line through the origin with the integral breadth  $\xi$  of the strain contribution as slope. However, particle size and strain broadening both can be present and anisotropic with diffraction order, which results in significant deviations/fluctuations in the Williamson-Hall plots. A straightforward solution can be to use the same set of reflection planes with several orders of reflection [14].

A variety of energetic materials has been investigated with this method, amongst them HMX, RDX, CL-20, FOX-7, FOX-12 and ADN [15,16] and the current results of TKX-50 are discussed in this context. Figure 6 shows the wedge-like scattering of a highly anisotropic structure. The distribution contains two pairs of peaks (020)/(040) and (011)/(022) that belong to the same set of reflections. The reciprocal peak widths of (020) and (040) arrange at the bottom of the distribution in the Williamson-Hall plot with a comparably low slope of 0,11 of the regression line, whereas the peaks (011) and (022) arrange at the upper rim of the distribution with a significantly higher slope of 0,32. Both lines intersect the y-axis at negative values, which physically does not make sense and seem to be attributed to the calibration procedure. It, however, is an indication for the absence of significant size broadening.

Hence, the Williamson-Hall analysis revealed that the (010)-layer structure shown in Figure 1 is not affected by significant micro strain or defects such as stacking faults. Such kind of layer structures were also reported for FOX-7 and ADN, where the layers are discussed to be responsible for the low sensitivity by providing slip systems for strain release, but on the other hand may cause mechanical and thermal stability problems when connected to high micro strains as reported for ADN [17]. Thus, the results give raise to the hypothesis that the layer structure support the low sensitivity of the energetic material but without impairment of its mechanical stability.

## 4 Conclusion

TKX-50 is in the focus of current investigations, with the object of developing new high-performance low sensitivity energetic formulations. Therefore, the thermal behavior of TKX-50 was reinvestigated over an extended temperature range. The investigations prove phase stability and volume continuance between  $-80$  and  $180 \text{ °C}$ , which should enclose most temperature requirements of future application scenarios. Besides, the micro structure of the TKX-50, synthesized at the Fraunhofer ICT, was analyzed and parameters are discussed to support a low sensitivity and mechanical stability of the substance. Hence, the detailed

characterization of the thermal expansion behavior and microstructure shall be used as a base for ongoing development, refinement and quality assessment of TKX-50 grades and TKX-50-containing products.

## Abbreviations

ABTOX	Diammonium 5,5'-bitetrazole-1,1'-diolate
ADN	Ammonium dinitramide
CCDC	Cambridge Crystallographic Data Centre
CL-20	Hexanitrohexaazaisowurtzitane
CSD	Cambridge Structural Database
CTEs	Coefficients of thermal expansion
FOX-12	Guarnyl ureadinitramide
FOX-7	1,1-Diamino-2,2-dinitroethylene
GAP	Glycidyl azide polymer
HMX	Cyclotetramethylene tetranitramine, high explosive
HTPB	Hydroxyl-terminated polybutadiene
ICT	Fraunhofer Institut für Chemische Technologie, Pfinztal, Germany
RDX	Cyclotrimethylene trinitramine, high explosive
SRM	Standard reference material
TGA-DSC	Thermogravimetry-differential scanning calorimetry
TKX-50	Dihydroxylammonium 5,5'-bistetrazole-1,1'-diolate
XRD	X-ray diffraction

## Data Availability Statement

No Data available.

## References

- [1] N. Fischer, D. Fischer, T. M. Klapötke, D. G. Piercey, J. Stierstorfer, Pushing the limits of energetic materials – the synthesis and characterization of dihydroxylammonium 5,5'-bistetrazole-1,1'-diolate, *J. Mat. Chem.* **2012**, *22*, 20418–20422.
- [2] T. M. Klapötke, T. G. Witkowski, Z. Wilk, J. Hadzik, Determination of the Initiating Capability of Detonators Containing TKX-50, MAD-X1, PETNC, DAAF, RDX, HMX or PETN as a Base Charge, by Underwater Explosion Test, *Propellants Explos. Pyrotech.* **2016**, *41*, 92–97.
- [3] T. G. Witkowski, *Synthesis, Characterization and Testing of Potential Energetic Materials*, Dissertation of Ludwig-Maximilians-Universität, München, Germany, **2017**.
- [4] N. Fischer, T. M. Klapötke, S. Matečić Mušanić, J. Stiersdorfer, M. Suceška, TKX-50, *16th Seminar on New Trends in Research of Energetic Materials*, Pardubice, Czech Republic, April 10–12, **2013**, 566–577.
- [5] Z. Lu, X. Xue, L. Meng, Q. Zeng, Y. Chi, G. Fan, H. Li, Z. Zhang, F. Nie, C. Zhang, Heat-Induced Solid-Solid Phase Transformation of TKX-50, *J. Phys. Chem. C* **2017**, *121*, 8262–8271.
- [6] J. Jia, Y. Liu, S. Huang, J. Xu, S. Li, H. Zhang, X. Cao, Crystal structure transformation and step-by-step thermal decomposition behavior of dihydroxylammonium 5,5'-bistetrazole-1,1'-diolate, *RSC Adv.* **2017**, *7*, 49105–49113.
- [7] Z. A. Dreger, A. I. Stas, Z.-G. Yu, Y.-S. Chen, Y. Tao, High-Pressure Structural Response of an Insensitive Energetic Crystal: Dihydroxylammonium 5,5'-Bistetrazole-1,1'-diolate (TKX-50), *J. Phys. Chem. C* **2017**, *121*, 5761–5767.
- [8] P. Gerber, Properties of Explosive Charges based on TKX-50, *16th International Detonation Symposium*, Cambridge, MD, USA, July 15–20, **2018**.
- [9] SRM 660a; *Lanthanum hexaboride Powder*; National Institute of Standards and Technology; U. S. Department of Commerce: Gaithersburg, MD, October 29, **2015**.
- [10] R. A. Young, Ed., *The Rietveld Method*, International Union of Crystallography, Oxford University Press, New York, **1995**.
- [11] *TOPAS 4.2*, Bruker AXS GmbH, Karlsruhe, Germany, **2009**.
- [12] G. K. Williamson, W. H. Hall, X-ray line broadening from filed aluminium and wolfram, *Acta Metall.* **1954**, *1*, 22–31.
- [13] J. I. Langford, Line Profile and Sample Microstructure, in: *Industrial Application of X-Ray Diffraction* (Eds.: F. H. Chung, D. K. Smith), Marcel Dekker, Inc., New York **2000**, p. 751.
- [14] T. Ungar, Warren-Averbach Applications, in: *Industrial Application of X-Ray Diffraction* (Eds.: F. H. Chung, D. K. Smith), Marcel Dekker, Inc., New York **2000**, p. 847.
- [15] M. Herrmann, U. Förter-Barth, P. B. Kempa, Size/strain diffraction peak broadening of the energetic materials HMX, CL-20 and FOX-12, *40th International Annual Conference of ICT, Energetic Materials - Characterization, Modelling and Validation*, Karlsruhe, Germany, June 23–26, **2009**, p. 32/1–11.
- [16] M. Herrmann, U. Förter-Barth, P. B. Kempa, Size/strain diffraction peak broadening of the energetic materials FOX-7, RDX and ADN, *Cent. Eur. J. Energ. Mater.* **2009**, *6*, 183–193.
- [17] M. Herrmann, U. Förter-Barth, P. B. Kempa, T. Heintz, Thermal Behavior of ADN and ADN-Prills – Crystal and Micro Structure – Part II, *49th International Annual Conference of ICT, Energetic Materials - Synthesis, Processing, Performance*, Karlsruhe, Germany, June 26–29, **2018**, p. 23/1–11.

Manuscript received: October 2, 2020

Revised manuscript received: November 13, 2020